Scattering time and single-particle relaxation time in a disordered two-dimensional electron gas

A. Gold

Groupe de Physique des Solides de l'Ecole Normale Supérieure, Université Paris 7, Tour 23, 2 place Jussieu, F-75251 Paris, France and Physik Department, Technische Universität München, D-8046 Garching, Federal Republic of Germany*

(Received 7 December 1987; revised manuscript received 9 March 1988)

We calculate the scattering time (which determines the conductivity) and the single-particle relaxation time (which determines the density of states) for a disordered two-dimensional electron gas in lowest order of the electron-impurity interaction. Analytical results and numerical results for remote impurity doping, homogeneous background doping, interface roughness scattering, and alloy disorder scattering in $In_{1-x}Ga_xAs$ quantum wells are presented. Self-consistency effects are also included and provide a theoretical frame for estimating the validity of the results calculated in lowest order of the electron-impurity interaction. A logarithmic singularity is found for the single-particle relaxation time in the case of homogeneous background doping.

I. INTRODUCTION

The electronic properties of two-dimensional electron gases are of fundamental importance to the understanding of Si metal-oxide–semiconductor (MOS) systems and the field-effect transistor based on $Al_xGa_{1-x}As/GaAs$ heterostructures of quantum wells. For a review see the article of Ando, Fowler, and Stern.[1]

Recently, it has been pointed out that there is a big difference between the scattering time, which determines the mobility of the disordered two-dimensional electron gas, and the single-particle relaxation time, which determines the density of states of the electron gas, in $Al_xGa_{1-x}As/GaAs$ heterostructures.[2] In Ref. 2 the single-particle relaxation time was named the "quantum lifetime." It was assumed that this quantum lifetime determines the magnitude of the Shubnikov–de Haas oscillations. Theoretical and experimental results on Si-MOS systems and $Al_xGa_{1-x}As/GaAs$ heterostructures were presented in Ref. 2. The difference between the two characteristic times is due to the fact that for long-ranged scattering potentials backscattering, which has the most effect on resistance (or scattering time), is suppressed,[3] and the scattering time is strongly enhanced in comparison to the single-particle relaxation time. The ratio of the scattering time to the single-particle relaxation time was found to be smaller than 1 for interface roughness scattering in Si-MOS systems,[2] in agreement with former experimental results.[4] For impurity scattering in $Al_xGa_{1-x}As/GaAs$ heterostructures the ratio of the transport time and the single-particle relaxation time was found to be much greater than 1,[2] in agreement with former experimental results on the same system.[5]

A clear definition of the single-particle relaxation time was given in Ref. 6. For three-dimensional systems the origin of the difference between the two characteristic times is well known, see Ref. 7, and the ratio in normal metals is close to 1. However, for remote doping the ratio between the scattering time and the single-particle relaxation time can be strongly enhanced.[6] This result is supported by experiments,[2,5,8] where the single-particle relaxation time was extracted from the magnitude of the Shubnikov–de Haas oscillations.

The magnetic field dependence of the single-particle relaxation time was neglected in these calculations.[6] However, the good agreement between theory and experiment suggests that the magnetic field dependence of the single-particle relaxation time might be small. Moreover, the single-particle relaxation time determines the density of states and is an important input parameter for theoretical calculations. For example, the effects of disorder on the screening properties of a disordered electron gas use the single-particle relaxation time as input. Theoretical results have been published for three-dimensional systems[9] and for two-dimensional systems.[10] The effects of disorder on the density of states were neglected in a theory on the metal-insulator transition in disordered electron gases given in Refs. 11 and 12. The metal-insulator transition in three-dimensional systems[11] and in two-dimensional systems[12] was discussed on this assumption. The calculation of the single-particle relaxation time offers the possibility of estimating the validity of this assumption.

In Ref. 6 only impurity scattering was discussed explicitly. For surface roughness scattering the ratio of the scattering time and the single-particle relaxation time was found to be close to 1.[2,4,6] In this paper we present analytical and numerical results on the scattering time and the single-particle relaxation time in Si-MOS systems, $Al_xGa_{1-x}As/GaAs$ heterostructures, and $InP/In_{1-x}Ga_xAs/InP$ quantum wells. The scattering mechanisms which we consider are ionized impurity scattering, homogeneous background scattering, interface roughness scattering, and alloy disorder scattering. We find that for certain interface-roughness parameters the ratio of the scattering time to the single-particle relaxation time can be strongly enhanced. The results for the different scattering mechanisms offer the possibility of determining the relevant scattering mechanisms in disordered two-dimensional electron gases. The lowest-order results in the electron-impurity interaction are extended to include self-consistency effects. Applying this theory, the validity range of the lowest-order result can be estimated.

The paper is organized as follows. In Sec. II we explain the model and the theoretical frame of our calculations. The results in the lowest order of the electron-impurity interaction are discussed in Sec. III. The self-consistent theory is presented in Sec. IV. In Sec. V we conclude. Aspects of alloy disorder scattering and of three-dimensional systems are discussed in the Appendix.

II. MODEL AND THEORY

In this section we explain the various scattering mechanisms and derive the general formulas for the scattering time and the single-particle relaxation time.

A. The scattering mechanisms

As usual, the disorder in the two-dimensional electron gas is characterized by the random potential $\langle |U(\mathbf{q})|^2\rangle$. q is the two-dimensional wave number. We assume that the electron gas can move in the xy plane and is confined in the z plane.

For a two-dimensional sheet of impurities with a two-dimensional impurity density n_i at a distance z_i from the electron gas (remote impurity doping) the random potential $U_1(\mathbf{q})$ is given by

$$\langle |U_1(\mathbf{q})|^2\rangle = n_i \left[\frac{2\pi e^2}{\epsilon_L}\frac{1}{q}\right]^2 F_R(q,z_i)^2 . \tag{1}$$

ϵ_L is the dielectric constant of the background. $F_R(q,z_i)$ is a form factor due to the distance z_i between the impurity layer and the electron gas and the finite extension of the electron gas in the z direction. For Si-MOS systems and $Al_xGa_{1-x}As/GaAs$ heterostructures the form factor can be found in Ref. 13, see also Ref. 1. For the form factor of quantum wells see the analytical results of Ref. 14. If the finite extension of the electron gas is neglected (for quantum well width $L=0$) one gets with $\alpha=|z_i|$ as the spacer thickness

$$F_R(q,\alpha)=e^{-2q\alpha} \tag{2}$$

and the electron gas is assumed to be at $z=0$.

For homogeneous background doping of the volume, characterized by the three-dimensional impurity density N_B, we get for quantum wells[14]

$$\langle |U_2(\mathbf{q})|^2\rangle = N_B L \left[\frac{2\pi e^2}{\epsilon_L}\frac{1}{q}\right]^2 F_B(q) . \tag{3}$$

L is the width of the quantum well and $F_B(q)$ is the form factor due to the finite extension of the electron gas. For $L\to 0$ we get

$$F_B(q)=\frac{1}{qL} \tag{4}$$

and the random potential does not depend on L.

Interface roughness scattering in Si-MOS systems[15] has been studied in detail, see Ref. 1. The random potential is written as

$$\langle |U_3(\mathbf{q})|^2\rangle = \pi\Delta^2\Lambda^2 q_s^2 \epsilon_F^2 \left[1+2\frac{N_D}{n}\right]^2 e^{-q^2\Lambda^2/4} . \tag{5}$$

Δ and Λ are the height and the length parameters of the interface roughness between the Si and the SiO_2. q_s is the Thomas-Fermi screening wave number, ϵ_F is the Fermi energy, n is the electron density and N_D is the depletion density. For quantum wells the random potential is given by[16]

$$\langle |U_3(\mathbf{q})|^2\rangle = 2\frac{\pi^5}{m_z^2}\frac{\Delta^2\Lambda^2}{L^6} e^{-q^2\Lambda^2/4} . \tag{6}$$

m_z is the mass perpendicular to the interface.

Alloy disorder scattering for heterostructures was considered first by Ando[17] for $Al_xGa_{1-x}As/GaAs$ heterostructures, where the alloy disorder is in the barrier ($Al_xGa_{1-x}As$) and later for $InP/In_{1-x}Ga_xAs$ heterostructures[18] and quantum wells,[19] where the alloy disorder produces stronger effects than in $Al_xGa_{1-x}As/GaAs$ due to the fact that the alloy disorder and the electron gas are not separated in space. For quantum wells with infinite barriers and the alloy disorder in the well we get for the random potential

$$\langle |U_4(\mathbf{q})|^2\rangle = x(1-x)\frac{a^3}{4}(\delta V)^2\frac{3}{2}\frac{1}{L} . \tag{7}$$

δV is the spatial average of the fluctuating alloy potential over the alloy unit cell and a^3 is the alloy unit cell.

The electron-electron interaction $V(q)$ is written as

$$V(q)=\frac{2\pi e^2}{\epsilon_L}\frac{1}{q}F_c(q) \tag{8}$$

and $F_c(q)$ is the form factor due to the finite extension of the electron gas in the z direction. $F_c(q)$ for Si-MOS systems and heterostructures was given in Ref. 13, see also Ref. 1. For quantum wells with infinite barriers see Ref. 14.

The dielectric function $\epsilon(q)$ of the electron gas is given by[20,21]

$$\epsilon(q)=1+V(q)[1-G(q)]X^0(q) . \tag{9}$$

$G(q)$ is the Hubbard form of the local field correction[21] and $X^0(q)$ is the polarizability of the two-dimensional electron gas.[20]

B. The scattering time

For a d-dimensional electron gas in the presence of disorder, characterized by $\langle |U(\mathbf{q})|^2\rangle$, the scattering time τ_t (which determines the mobility $\mu=e\tau_t/m^*$, m^* being the mass in the xy direction) is expressed as[12]

$$\frac{1}{\tau_t}=\frac{1}{dn\,m^*}\sum_{\mathbf{q}} q^2\frac{\langle |U(\mathbf{q})|^2\rangle}{\epsilon(q)^2}\Phi''(\mathbf{q},0) . \tag{10}$$

Planck's constant $\hbar$ is set equal to 1 in this paper. $\Phi''(\mathbf{q},0)$ is the density-density relaxation function of the noninteracting electron gas and is proportional to the Lindhard function for $d=3$.[22] For $d=2$ see Ref. 20. Equation (10) is for zero temperature.

For two-dimensional systems one gets the equivalent of the Stern-Howard formula[13]

$$\frac{1}{\tau_t}=\frac{1}{2\pi\varepsilon_F}\int_0^{2k_F}dq\frac{q^2}{(4k_F^2-q^2)^{1/2}}\frac{\langle\,|U(\mathbf{q})|^2\rangle}{\epsilon(q)^2}\ , \tag{11}$$

where k_F is the Fermi wave number.

Equations (10) and (11) are the lowest-order results for the scattering time. This means that $1/\tau_t$ is linear in the random potential (linear in n_i for remote impurity scattering). If multiple scattering effects are taken into account, τ_{tr} (the index r indicates renormalized) is reduced in comparison to the lowest-order calculation and goes to zero at the metal-insulator transition.[11,12,16] Weak localization effects[23] were neglected in this approach, see the discussion in Ref. 12. For details of the theory on multiple scattering effects, see Ref. 12. The basic idea in this theory on multiple scattering effects is that due to disorder, the propagation of density fluctuations is changed and the impurity-renormalized density-density correlation function, depending itself on τ_{tr}, must be used on the right-hand side of Eq. (10). Numerical results of this theory will be presented in Sec. IV.

C. The single-particle relaxation time

The one-electron properties of the interacting electron system are described by the one-electron Green's function $G(\mathbf{k},E)$. $\mathbf{k}$ and E are the wave vector and the energy of the quasiparticle. The Green's function is expressed as[7]

$$G(\mathbf{k},E)=\frac{1}{E-k^2/2m^*-\Sigma(\mathbf{k},E)}\ . \tag{12}$$

The self-energy $\Sigma(\mathbf{k},E)$ is a sum of the electron-electron interaction contribution (exchange and correlation) and the electron-disorder interaction. We neglect the first part in this paper because it does not depend on disorder and gives rise to a rigid shift of the band. It is assumed that the subband energy of the lowest subband is at $E=0$.

In the third Klauder approximation[24] the self-energy due to the disorder is written as

$$\Sigma(\mathbf{k},E)=\sum_{\mathbf{q}}\frac{\langle\,|U(\mathbf{q})|^2\rangle}{\epsilon(q)^2}G(\mathbf{q}+\mathbf{k},E)\ . \tag{13}$$

The third Klauder approximation was compared with the best, the fifth, Klauder approximation in Ref. 25 for three-dimensional systems and in Ref. 26 for two-dimensional systems. It was shown that the third Klauder approximation gives a fair description of the density of states, given by

$$\sigma(E)=\mp\sum_{\mathbf{k}}\frac{1}{\pi}\mathrm{Im}G(\mathbf{k},E\pm i0)\ , \tag{14}$$

if impurity bands can be neglected. This is the case for high impurity density, where the impurity band has merged with the conduction band, and for high electron density, where the Fermi energy is in the conduction band. Equation (13) represents the self-consistent Born approximation and multiple scattering effects are included in this approximation, because $G(\mathbf{k},E)$ depends on $\Sigma(\mathbf{k},E)$. The second Klauder approximation is the zero-order result (linear in the disorder) of the third Klauder approximation and is given by

$$\Sigma(\mathbf{k},E)=\sum_{\mathbf{q}}\frac{\langle\,|U(\mathbf{q})|^2\rangle}{\epsilon(q)^2}\frac{1}{E-(\mathbf{q}+\mathbf{k})^2/2m^*}\ . \tag{15}$$

In the mass-shell approximation one calculates $\Sigma(k=k_F,E=\varepsilon_F)$. The Green's function in Eq. (15) [the final part of Eq. (15)] provides a δ function and one integration of the two-dimensional $\mathbf{q}$ integral can be performed easily. The single-particle relaxation time $\tau_s(\mathbf{k},E)$ is defined by[7] $\Sigma''(\mathbf{k},E)=1/2\tau_s(\mathbf{k},E)$. For $d=2$ we get with Eq. (15) in the mass-shell approximation [$\tau_s\equiv\tau_s(k_F,\varepsilon_F)$]

$$\frac{1}{\tau_s}=\frac{1}{2\pi\varepsilon_F}\int_0^{2k_F}dq\frac{2k_F^2}{(4k_F^2-q^2)^{1/2}}\frac{\langle\,|U(\mathbf{q})|^2\rangle}{\epsilon(q)^2}\ . \tag{16}$$

This is the expression of the single-particle relaxation time, which will later be discussed in detail for the various scattering mechanisms. Equation (16) is equivalent to formulas derived in Refs. 2 and 6. The difference between the scattering time, Eq. (11), and the single-particle relaxation time, Eq. (16), is obvious. $2k_F^2$ in Eq. (16) is replaced by $q^2=2k_F^2(1-\cos\theta)$ in Eq. (11); θ is the scattering angle of the electron.

For the self-consistent theory we replace in the Green's function on the right-hand side of Eq. (13) $\Sigma(\mathbf{k}+\mathbf{q},E)$ by $\Sigma(\mathbf{k},E)$. This approximation means that within the power series

$$\Sigma(\mathbf{k}+\mathbf{q},E)=\Sigma(\mathbf{k},E)+[d^2\Sigma(\mathbf{k}+\mathbf{q},E)/dq^2]_{q=0}q^2+O(q^4)$$

only the first term is considered. Within the mass-shell approximation $\Sigma(k,E)=\Sigma(k_F,\varepsilon_F)$ (Ref. 7) and with $\Sigma(k_F,\varepsilon_F)=i/2\tau_{sr}(k_F,\varepsilon_F)$ (the index r indicates renormalized) one gets for the third Klauder approximation, Eq. (13), for $d=2$ with $\tau_{sr}\equiv\tau_{sr}(k_F,\varepsilon_F)$,

$$\frac{1}{\tau_{sr}}=\frac{2m^*}{\pi^2}\int_0^\infty dq\,q\frac{\langle\,|U(\mathbf{q})|^2\rangle}{\epsilon(q)^2}\times\int_{-1}^{1}\frac{dy}{(1-y^2)^{1/2}}\times\frac{m^*/\tau_{sr}}{(q^2+2k_Fqy)^2+(m^*/\tau_{sr})^2}\ . \tag{17}$$

The square-root singularity for $y=+1$ and $y=-1$ contributes most efficiently to the integral over y in Eq. (17) and a rough estimate for Eq. (17) is written as

$$\frac{1}{\tau_{sr}}=\frac{m^*}{\pi}\int_0^\infty dq\,q\frac{\langle\,|U(\mathbf{q})|^2\rangle}{\epsilon(q)^2}\times\left[\frac{m^*/\tau_{sr}}{(q^2-2qk_F)^2+(m^*/\tau_{sr})^2}+\frac{m^*/\tau_{sr}}{(q^2+2qk_F)^2+(m^*/\tau_{sr})^2}\right]\ . \tag{18}$$

Equation (18) will be discussed in Sec. IV. It represents a generalization of the lowest-order result, Eq. (16), by taking into account multiple scattering effects.

D. Parameters

For discussion of real systems we have to specify the model parameters. For Si-MOS systems we use $m^*=0.19m_0$, $m_z=0.96m_0$, $\epsilon_L=7.7$, and $g_v=2$. m_0 is the vacuum mass of the electron and g_v is the valley degeneracy. The $Al_xGa_{1-x}As/GaAs$ heterostructure is parametrized by $m^*=m_z=0.067m_0$, $\epsilon_L=12.8$, and $g_v=1$. We use $m^*=m_z=0.041m_0$, $\epsilon_L=13.3$, and $g_v=1$ for $In_{1-x}Ga_xAs$ quantum wells with $x=0.47$. For the alloy unit cell we use $a=5.9$ Å.

The scattering time for Si quantum wells was discussed in Ref. 14. However, these results cannot be used to describe the mobility of $In_{1-x}Ga_xAs$ quantum wells quantitatively. The reason is the following: we will see later that $2k_F/q_s$ is an important parameter of the transport theory and this parameter differs greatly in Si and $In_{1-x}Ga_xAs$ quantum wells. For $2k_F=q_s$ the density dependence of the mobility changes, see Ref. 14. The relation $2k_F=q_s$ defines an electron density $n^*=g_vq_s^2/(8\pi)$. For Si-MOS systems, $Al_xGa_{1-x}As/GaAs$ heterostructure, and $In_{1-x}Ga_xAs$ quantum wells we get $n^*=2.8\times10^{13}$ cm^{-2}, 1.6×10^{11} cm^{-2}, and 5.4×10^{10} cm^{-2}, respectively.

III. RESULTS AND DISCUSSION: LOWEST-ORDER THEORY

In this section we present analytical and numerical results for the scattering time τ_t, Eq. (11), the single-particle relaxation time τ_s, Eq. (16), and the ratio τ_t/τ_s in case of the various scattering mechanisms. Si-MOS systems, $Al_xGa_{1-x}As/GaAs$ heterostructures, and $In_{1-x}Ga_xAs$ quantum wells are considered.

A. Analytical results

The square root singularity at $q=2k_F$ in Eqs. (11) and (16) can be used in case of $4k_F|z_i|\ll1$ to derive analytical results for the scattering time and the single-particle relaxation time for remote-impurity doping, see Eq. (1). Detailed results for τ_t can be found in Ref. 27 for Si-MOS systems and in Ref. 14 for quantum wells. In Ref. 27 it was shown that the analytical results are exact in the limit $n\to0$. For finite electron density the analytical results on the scattering time are somewhat lower than the numerical results, see Fig. 1 in Ref. 27. The random potential is characterized by the $q\to0$ behavior, $\lim_{q\to0}\langle|U(\mathbf{q})|^2\rangle\propto q^\beta$. It was found that the analytical results become better in comparison to the numerical results for higher β values. The various scattering mechanisms are characterized by $\beta=-2$ for remote-impurity doping, $\beta=-3$ for homogeneous background doping, and $\beta=0$ for interface-roughness scattering and alloy disorder scattering.

For $4k_F|z_i|\gg1$, in case of remote-impurity scattering, or for $k_F\Lambda\gg1$, in case of interface-roughness scattering, the square root singularity in Eqs. (11) and (16) can be neglected and the approximation $(4k_F^2-q^2)^{1/2}\approx2k_F$ is used for the calculation of the q integral.

For remote impurity doping with $4k_F|z_i|\ll1$ we get

$$\frac{1}{\tau_t}=\frac{1}{\tau_s}=\epsilon_F\frac{\pi}{g_v}\frac{n_i}{n}\frac{F_R(2k_F,z_i)^2}{\{[1-G(2k_F)]F_c(2k_F)+2k_F/q_s\}^2}\ , \tag{19a}$$

and

$$\frac{\tau_t}{\tau_s}=1 \tag{19b}$$

holds for $k_F\to0$. According to our discussion on the accuracy of the analytical results we expect that for finite electron density the relation $\tau_t/\tau_s>1$ holds. For $4k_F|z_i|\gg1$ we get with $F_R(q,z_i)^2=e^{-2q|z_i|}f(q)^2$

$$\frac{1}{\tau_t}=\epsilon_F\frac{1}{g_v}\frac{n_i}{n}\frac{1}{(2k_F|z_i|)^3}\times\frac{f(1/2|z_i|)^2}{\{[1-G(1/2|z_i|)]F_c(1/2|z_i|)+1/2|z_i|q_s\}^2}\ , \tag{20a}$$

$$\frac{1}{\tau_s}=\epsilon_F\frac{1}{g_v}\frac{n_i}{n}\frac{1}{2k_F|z_i|}\times\frac{f(1/2|z_i|)^2}{\{[1-G(1/2|z_i|)]F_c(1/2|z_i|)+1/2|z_i|q_s\}^2}\ , \tag{20b}$$

and

$$\frac{\tau_t}{\tau_s}=(2k_F|z_i|)^2\ . \tag{20c}$$

For an ideally two-dimensional electron gas with $f(q)=1$ and for $G=0$ we get with Eq. (20a) (Ref. 28)

$$\frac{1}{\tau_t}=\epsilon_F\frac{1}{g_v}\frac{n_i}{n}\frac{1}{(2k_F\alpha)^3}\ . \tag{21}$$

For fixed n_i ($Al_xGa_{1-x}As/GaAs$ heterostructures with a gate) one expects for $4k_F\alpha\gg1$, $\mu\approx n^{3/2}$. The strong enhancement of τ_t/τ_s, Eq. (20c), in comparison to 1 was found numerically in Ref. 6.

For homogeneous background doping we get[29]

$$\frac{1}{\tau_t}=\epsilon_F\frac{2}{g_v}\frac{N_BL}{n}\frac{F_B(2k_F)}{\{[1-G(2k_F)]F_c(2k_F)+2k_F/q_s\}^2}\ . \tag{22}$$

For an ideal electron gas and $G=0$ we derive $1/\tau_t=\epsilon_FN_B/(g_vnk_F)$. The zero-order result for the single-particle relaxation time for homogeneous background doping does not exist. We find $\lim_{q\to0}\langle|U_2(\mathbf{q})|^2\rangle/\epsilon(q)^2\propto1/q$ and the q integral in Eq. (16) for the single-particle relaxation time is diverging because of an infrared singularity of the integral. This result indicates the failure of the lowest-order theory in the case of homogeneous background doping. A multiple scattering theory (or renormalized theory) has to be used to calculate τ_{sr}, see Sec. IV. Equation (20c) already indi-

cates this singularity.

The analytical results on τ_t in the case of interface-roughness scattering were given in Ref. 27 for Si-MOS systems and in Ref. 14 for quantum wells. For quantum wells we derive for $k_F\Lambda \ll 1$

$$\frac{1}{\tau_s}=\varepsilon_F 8\pi^5 \frac{\Delta^2\Lambda^2}{L^6 q_s^2}\frac{m^{*2}}{m_z^2}\frac{1}{\{[1-G(2k_F)]F_c(2k_F)+2k_F/q_s\}^2} \tag{23a}$$

and for $k_F\Lambda \gg 1$

$$\frac{1}{\tau_s}=\varepsilon_F 8\pi^{9/2}\frac{\Delta^2}{L^6\Lambda q_s^2 k_F^3}\frac{m^{*2}}{m_z^2} \times\frac{1}{\{[1-G(2/\Lambda)]F_c(2/\Lambda)+2/\Lambda q_s\}^2} . \tag{23b}$$

The ratio for τ_t/τ_s is given by

$$\frac{\tau_t}{\tau_s}=\begin{cases}\frac{2}{3}, & k_F\Lambda \ll 1\\ (k_F\Lambda)^2/3, & k_F\Lambda \gg 1 .\end{cases} \tag{23c}$$

Equation (23c) also holds for Si-MOS systems and heterostructures. In very high mobility samples of $Al_xGa_{1-x}As/GaAs$ heterostructures[30] an enhancement $\tau_t/\tau_s \gg 1$ could be due to remote-impurity scattering and (or) interface-roughness scattering. The density dependence of τ_t/τ_s cannot be used to distinguish between the two possibilities.

For alloy disorder scattering we get

$$\frac{1}{\tau_t}=\varepsilon_F\frac{9}{16}\frac{\delta V^2}{\varepsilon_F^2}\frac{k_F^2}{q_s^2}\frac{a^3k_F^2}{L}x(1-x) \times\frac{1}{\{[1-G(2k_F)]F_c(2k_F)+2k_F/q_s\}^2} . \tag{24a}$$

and we derive

$$\frac{1}{\tau_t}\propto\begin{cases}n, & n\to 0\\ \text{constant}, & n\to\infty .\end{cases} \tag{24b}$$

The single-particle scattering time is given by

$$\tau_s=\tfrac{3}{2}\tau_t . \tag{24c}$$

According to our remarks on the accuracy of the analytical results we conclude that for finite n we get $\tau_t/\tau_s > \frac{2}{3}$.

B. Si-MOS structures

The relevant scattering mechanisms for Si-MOS systems are well understood.[1] Measurements on τ_t (mobility) and on τ_s and a comparison to theory could be used to clarify whether τ_s could indeed be extracted from the amplitudes of the Shubnikov–de Haas oscillations. Multiple scattering effects can drastically reduce the scattering time in Si-MOS samples with low electron densities and with low peak mobility.[12,31] Such effects are probably important to the interpretation of the experimental results on Si-MOS systems.[2,4] Via mobility measurements the scattering parameters can be fixed by comparison to theory. The prediction of τ_t/τ_s from theory and the comparison to experimental results can be applied to test multiple scattering effects, see Sec. IV.

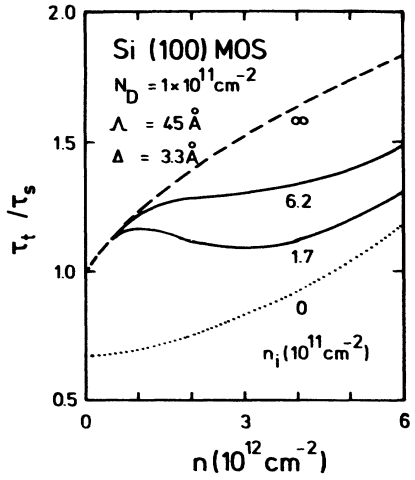

FIG. 1. Ratio of scattering time τ_t and single-particle relaxation time τ_s vs electron density n for Si(100)-MOS systems according to Eqs. (11) and (16). Remote impurity doping ($z_i=0$) (dashed line) and surface roughness scattering (dotted line) are included. The solid lines are for both scattering mechanisms and different impurity density n_i.

In Fig. 1 we show numerical results on τ_t/τ_s versus electron density for a Si-MOS structure. Impurity scattering (with impurities at the interface of Si/SiO_2) and surface-roughness scattering were taken into account. Experimental results on the mobility were given in Ref. 32, while the parameters of the interface-roughness scattering were derived in Ref. 33 by an adjustment of theoretical results on the mobility to the experimental results. The analytical results, Eqs. (19b) and (23c) on surface-roughness scattering and impurity scattering, respectively, are visible in Fig. 1 for $n\to 0$.

C. $Al_xGa_{1-x}As/GaAs$ heterostructures

Results on μ and τ_t/τ_s for an ideally two-dimensional electron gas in a $Al_xGa_{1-x}As/GaAs$ heterostructure in the presence of remote impurity scattering are shown in Fig. 2. The analytical results according to Eqs. (20c) and (21) are the dotted and the dashed lines. Figure 2 demonstrates the accuracy of our analytical results and the strong increase in τ_t/τ_s with increasing α.[6]

According to Eq. (21) we find for $n_i=n$

$$\mu/n^{3/2}=[6.1\times10^{16}/(\text{V s})]g_v^{1/2}\alpha^3/n . \tag{25}$$

For the very high mobility sample[30] with $\mu=5\times10^6$ $cm^2/V s$, $n=1.6\times10^{11}$ cm^{-2}, and $\alpha=750$ Å we get $\mu/n^{3/2}=1.6\times10^{-10}$ $cm^5/V s$. The experimental value was 0.75×10^{-10} $cm^5/V s$, see Fig. 3 of Ref. 30. We believe that interface roughness scattering cannot be neglected in heterostructures with such a high mobility. It is generally believed that interface roughness scattering

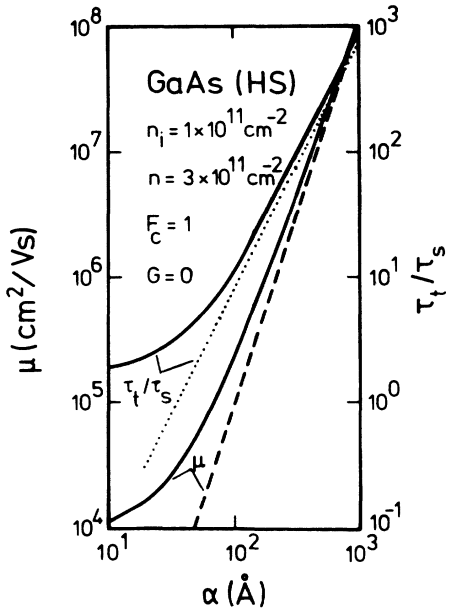

FIG. 2. Mobility μ and τ_t/τ_s vs spacer thickness α for an $Al_xGa_{1-x}As/GaAs$ heterostructure (HS) according to Eqs. (11) and (16) (solid lines). Finite thickness effect and local field corrections are neglected. The dashed and dotted lines are analytical results according to Eqs. (21) and (20c), respectively ($|z_i| = \alpha$).

is unimportant in $Al_xGa_{1-x}As/GaAs$ heterostructures.[34] However, it has been shown recently that interface-roughness scattering is the most important scattering mechanism in thin AlAs/GaAs/AlAs (Ref. 35) and in $Al_xGa_{1-x}As/GaAs/Al_xGa_{1-x}As$ (Ref. 36) quantum wells. The surface roughness parameters were determined to be $\Delta = 3$ Å, $\Lambda = 70$ Å (Ref. 35) and $\Delta = 2.4$ Å, $\Lambda = 65$ Å.[36] From the experimental data it is not clear whether the "normal" interface ($Al_xGa_{1-x}As/GaAs$) contributes to the scattering or whether all scattering comes from the "inverted" interface ($GaAs/Al_xGa_{1-x}As$). However, the above-mentioned interface-roughness parameters, applied to the normal interface, suggest that interface-roughness scattering is important in the high mobility sample of Ref. 30. For a recent review (from theoretical and experimental points of view) on the mobility of $Al_xGa_{1-x}As/GaAs$ heterostructures see Ref. 37.

D. InGaAs quantum wells

In this section we present the results on $InP/In_{1-x}Ga_xAs/InP$ quantum wells and the various scattering mechanisms. We discuss the mobility and τ_t/τ_s vs electron density. The quantum well interfaces are assumed to be at $z = 0$ and $z = L$, see Fig. 1 of Ref. 14.

The results on an $L = 100$-Å quantum well and a remote doping are shown in Fig. 3. From the numerical results we find the relation

$$\mu \propto n^{1.7}/n_i \tag{26}$$

and with increasing spacer thickness the mobility increases. In a simple model, one has to assume that $n_i = n$ and the mobility has to be rescaled according to this relation. The results on τ_t/τ_s do not depend on this model assumption. For $n \to 0$ we find $\tau_t/\tau_s = 1$, see Eq. (19b), while for $n \gg 10^{11}$ cm^{-2} we find $\tau_t/\tau_s \propto n$, in agreement with Eq. (20c).

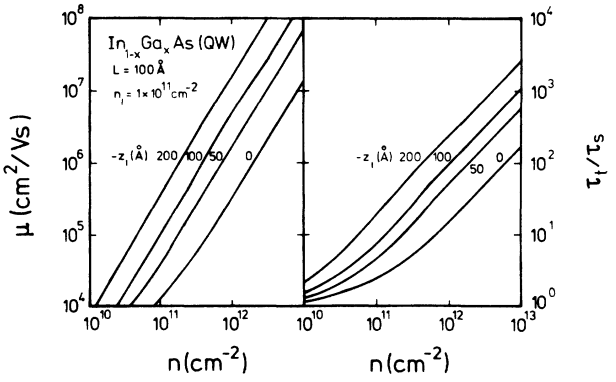

FIG. 3. Mobility μ and τ_t/τ_s vs electron density n for remote doping in an $In_{1-x}Ga_xAs$ quantum well (QW) according to Eqs. (11) and (16). Results for various values of z_i are shown, see Eq. (1).

For background impurity scattering our results on the mobility are shown in Fig. 4. The numerical results on $n > 10^{11}$ cm^{-2} can be written as

$$\mu = \left[9.5\times10^5\ \frac{\text{cm}^2}{\text{Vs}}\right]\left[\frac{1\times10^{16}\ \text{cm}^{-3}}{N_B}\right] \times \left[\frac{n}{10^{12}\ \text{cm}^{-2}}\right]^{1.4} . \tag{27}$$

Local field corrections reduce the screening properties of the electron gas and the mobility is reduced; however, they are unimportant for high electron density, see Fig. 4.

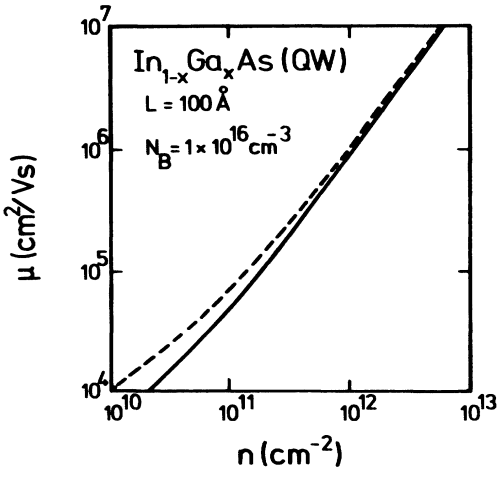

FIG. 4. Mobility μ vs density n for homogeneous background doping in an $In_{1-x}Ga_xAs$ quantum well according to Eq. (11). Local field effects are neglected for the dashed line.

We mention that there is only a very weak L dependence observed for homogeneous background doping, see also Fig. 3 in Ref. 16. The result on the single-particle relaxation time is discussed in Sec. IV.

Our results for interface roughness scattering are shown in Fig. 5. The mobility scales according to Ref. 16: $\mu \propto L^6$. For $k_F \Lambda > 1$ backscattering is reduced and the mobility increases with increasing electron density.[14] We find $\mu \propto m_z^2$ and interface-roughness scattering in $In_{1-x}Ga_xAs$ quantum wells is increased by a factor of 2.6 in comparison to GaAs quantum wells. For high electron density we find $\tau_t/\tau_s \propto n$, and for $n \to 0$ we get $\tau_t/\tau_s = \frac{2}{3}$. These asymptotic results, according to Eq. (23c), are also shown in Fig. 5 as dotted and dashed lines.

For alloy disorder scattering our results are shown in Fig. 6. The asymptotic behavior, according to Eq. (24b) for the mobility and to Eq. (24c) for τ_t/τ_s, can be seen in Fig. 6. Most important is the very weak density dependence of τ_t/τ_s. The dashed line represents the mobility for an unscreened alloy disorder scattering potential, see the discussion in the Appendix.

From our analysis of the four scattering mechanisms discussed in connection with Figs. 3–6 we conclude that for $n > 5\times 10^{11}$ cm^{-2} alloy disorder scattering is probably the dominant scattering mechanism. For $n < 5\times 10^{11}$ cm^{-2} remote doping or homogeneous background doping is expected to be important as well. Of course, in thin quantum wells interface-roughness scattering will dominate. The dependence of the mobility on the quantum well width, which is given by

$$\mu \propto \begin{cases} L^0 & \text{(homogeneous background doping)} \\ L^1 & \text{(alloy disorder scattering)} \\ L^6 & \text{(interface-roughness scattering)}, \end{cases} \tag{28}$$

could help to get a better understanding on the importance of the various scattering mechanisms in real $In_{1-x}Ga_xAs$ quantum wells.[38–42] The L dependence for remote-impurity doping is more complex. For $|z_i| \gg L$ only a weak L dependence in the mobility exists, whereas for doping in the quantum well a stronger L dependence is found.

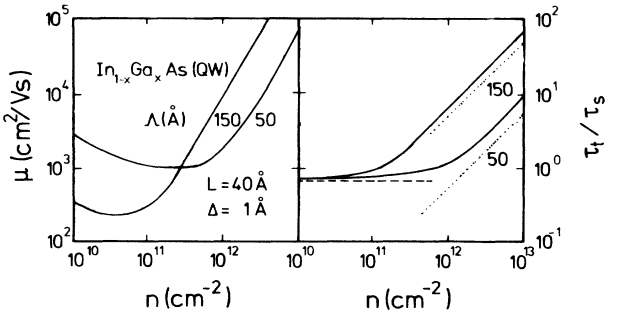

FIG. 5. Mobility μ and τ_t/τ_s vs electron density n for interface roughness scattering in an $In_{1-x}Ga_xAs$ quantum well according to Eqs. (11) and (16) as the solid lines. The dotted and dashed lines represent the analytical results, see Eq. (23c).

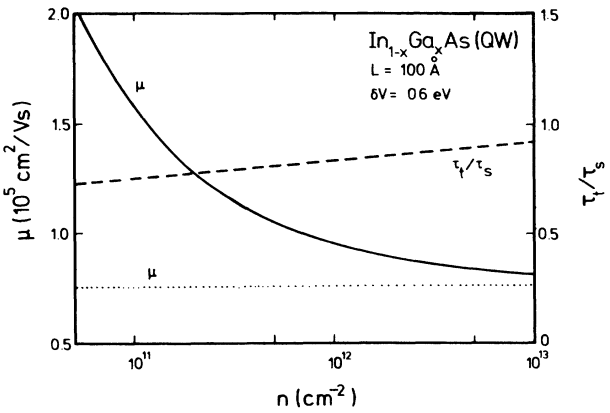

FIG. 6. Mobility μ and τ_t/τ_s vs electron density n for alloy disorder scattering in an $In_{1-x}Ga_xAs$ quantum well according to Eqs. (11) and (16). For the dotted line screening was neglected, see Eq. (A1).

Our results on τ_t/τ_s for remote-impurity doping and interface-roughness scattering demonstrate that $\tau_t/\tau_s \gg 1$ is only a necessary but not a sufficient condition for scattering due to remote-impurity doping. Combined measurements of τ_t and τ_s versus electron density and for various quantum well widths are necessary to get a good idea of the relevant scattering mechanism.

IV. RESULTS AND DISCUSSION: SELF-CONSISTENT THEORY

In this section we calculate the single-particle relaxation time and the scattering time by taking into account multiple scattering effects.

A. The single-particle relaxation time: short-range potentials

In Sec. III we found that the single-particle relaxation time for homogeneous background scattering does not exist in the zero-order theory. An approximative expression for the (self-consistent) third Klauder approximation in mass-shell approximation was given in Eq. (18). First we calculate the single-particle relaxation time for those scattering potentials, where the zero-order result exists.

The factor $1/[q^2(q-2k_F)^2+(m^*/\tau_{sr})^2]$ in Eq. (18) peaks for $q=0$ and $q=2k_F$. Because of the q prefactor in Eq. (18) the peak at $q=0$ can be neglected in a simple estimate of the integral. We write for Eq. (18)

$$\frac{1}{\tau_{sr}} = \frac{m^*}{\pi} C \frac{\langle |U(2k_F)|^2 \rangle}{\epsilon(2k_F)^2} \times \int_0^\infty dq\, q \frac{m^*/\tau_{sr}}{(q^2-2qk_F)^2+(m^*/\tau_{sr})^2} . \tag{29}$$

The coefficient C accounts for this rough estimation and is specified later. The q integral in Eq. (29) is further simplified. With $x = q - 2k_F$ we only take into account the most singular part at $x=0$ and get

$$\frac{1}{\tau_{sr}}=\frac{m^*}{\pi}C\frac{\langle\,|\,U(2k_F)\,|^2\rangle}{\epsilon(2k_F)^2}\times\int_{-2k_F}^{\infty}dy\,2k_F\frac{m^*/\tau_{sr}}{(2k_Fy)^2+(m^*/\tau_{sr})^2}\ . \tag{30}$$

We replace the upper integration boundary ∞ by $2k_F$ and calculate the elementary integral:

$$\frac{1}{\tau_{sr}}=\frac{2m^*}{\pi}C\frac{\langle\,|\,U(2k_F)\,|^2\rangle}{\epsilon(2k_F)^2}\arctan(8\varepsilon_F\tau_{sr})\ . \tag{31}$$

With Eq. (7) we derive for alloy disorder scattering

$$\frac{1}{\tau_{sr}}=\varepsilon_F\frac{3}{4\pi}\frac{\delta V^2}{\varepsilon_F^2}\frac{k_F^2}{q_s^2}\frac{a^3k_F^2}{L}x(1-x)\times\frac{\arctan(8\varepsilon_F\tau_{sr})}{\{[1-G(2k_F)]F_C(2k_F)+2k_F/q_s\}^2}\ , \tag{32}$$

where we have used $C=\frac{1}{2}$. Now we discuss the asymptotic behavior of Eq. (32). For $8\varepsilon_F\tau_{sr}\gg1$ we get

$$\frac{1}{\tau_{sr}}=\varepsilon_F\frac{3}{8}\frac{\delta V^2}{\varepsilon_F^2}\frac{k_F^2}{q_s^2}\frac{a^3k_F^2}{L}x(1-x)\times\frac{1}{\{[1-G(2k_F)]F_c(2k_F)+2k_F/q_s\}^2} \tag{33a}$$

and for $8\varepsilon_F\tau_{sr}\ll1$ we get

$$\frac{1}{\tau_{sr}}=\varepsilon_F\left[\frac{6}{\pi}\right]^{1/2}\frac{\delta V}{\varepsilon_F}\frac{k_F}{q_s}\left[\frac{a^3k_F^2}{L}x(1-x)\right]^{1/2}\times\frac{1}{[1-G(2k_F)]F_C(2k_F)+2k_F/q_s}\ . \tag{33b}$$

Equation (33a) is the zero-order result given in Eq. (24a) and the coefficient $C=\frac{1}{2}$ was chosen to get the same prefactor in Eq. (33a) as in Eq. (24a). The strong coupling result, Eq. (33b), can be written as

$$\frac{1}{\tau_{sr}}=\frac{1}{\tau_s}\left[\frac{16}{\pi}\varepsilon_F\tau_s\right]^{1/2}\ll\frac{1}{\tau_s} \tag{34}$$

and τ_s is the zero-order result, Eq. (24a). With Eq. (32) we can calculate next-order corrections to the lowest-order result. For alloy disorder scattering we get

$$\tau_{sr}=\tau_s\left[1+\frac{1}{4\pi}\frac{1}{\varepsilon_F\tau_s}+O(1/\varepsilon_F^2\tau_s^2)\cdots\right] \tag{35}$$

and we find that the zero-order result overestimates the effects of disorder, see also Eq. (34).

For interface-roughness scattering (with $k_F\Lambda\ll1$) and for remote-impurity scattering (with $4k_F\,|\,z_i\,|\ll1$) we get a similar result as for alloy disorder, namely,

$$\frac{1}{\tau_{sr}}=\frac{1}{\tau_s}\frac{2}{\pi}\arctan(8\varepsilon_F\tau_{sr})\ . \tag{36}$$

τ_s is the zero-order result on interface-roughness scattering, Eq. (23a), or for remote-impurity doping, Eq. (19a). Accordingly, Eqs. (34) and (35) also hold for these two scattering mechanisms. For remote impurity doping we have to choose $C=1$ to get the zero-order result [Eq. (23a)] for a weak electron-impurity coupling.

B. Single-particle relaxation time: background doping

A similar calculation as in Sec. IV A can be made in case of homogeneous background doping. We divide in Eq. (17) the integration over $-1\le y\le1$ into integrations over $-1\le y\le-1/2$, $-1/2\le y\le1/2$, and $1/2\le y\le1$. For the first and third regime of integration we consider the square root singularity for $y=-1$ and $y=1$, respectively, see Eq. (18). For the second regime of integration ($-1/2\le y\le1/2$) we replace $1/(1-y^2)^{1/2}$ by 1. Within these approximations we get

$$\frac{1}{\tau_{sr}}=\varepsilon_F\frac{1}{3g_v}\frac{N_BL}{n}\frac{1}{k_F^2}\int_0^{\infty}dq\frac{F_B(q)}{\{[1-G(q)]F_c(q)X^0(q)\varepsilon_F/n+q/q_s\}^2}\Omega(q) \tag{37a}$$

and

$$\Omega(q)=\frac{q/\varepsilon_F\tau_{sr}}{(q^2/k_F^2-2q/k_F)^2+(1/2\varepsilon_F\tau_{sr})^2}+\frac{q/\varepsilon_F\tau_{sr}}{(q^2/k_F^2+2q/k_F)^2+(1/2\varepsilon_F\tau_{sr})^2}$$
$$+\frac{3}{\pi}k_F\{\arctan[4\varepsilon_F\tau_{sr}q(1+q/k_F)/k_F]+\arctan[4\varepsilon_F\tau_{sr}q(1-q/k_F)/k_F]\}\ . \tag{37b}$$

The first and second functions in Eq. (37b) exhibit in the case of $4\varepsilon_F\tau_{sr}\gg1$ well-defined peaks at $q=-2k_F$, $q=0$, and $q=2k_F$. The integration is performed in the same approximation as discussed before and we derive for $4\varepsilon_F\tau_{sr}\gg1$

$$\frac{1}{\tau_{sr}}=\varepsilon_F\frac{\pi}{3g_v}\frac{N_B L}{n}\left[\frac{1}{k_F L}+\left[1+\frac{2}{\pi}\arctan(8\varepsilon_F\tau_{sr})\right]\frac{F_B(2k_F)}{\{[1-G(2k_F)]F_c(2k_F)+2k_F/q_s\}^2}\right.$$
$$+\frac{3}{\pi^2}\frac{1}{k_F}\int_0^\infty dq\frac{F_B(q)}{\{[1-G(q)]F_c(q)X^0(q)\varepsilon_F/n+q/q_s\}^2}$$
$$\left.\times\{\arctan[4\varepsilon_F\tau_{sr}q(1+q/k_F)/k_F]+\arctan[4\varepsilon_F\tau_{sr}q(1-q/k_F)/k_F]\}\right]. \quad (37c)$$

If we use $1/\varepsilon_F\tau_{sr}=0$ on the right-hand side of Eq. (37c) we get the (divergent) zero-order result. In this case the expression $\arctan(\cdots 1+q\cdots)+\arctan(\cdots 1-q\cdots)$ is (for $q>0$) given by $\theta(k_F-q)$ and for $q\to 0$ the integral is divergent. In Eq. (37c) the $k_F\le q\le 2k_F$ contribution to the lowest-order result is the term containing $F_B(2k_F)$.

For $1/\varepsilon_F\tau_{sr}\to 0$ we get from Eq. (37c)

$$\frac{1}{\varepsilon_F\tau_{sr}}=\frac{\pi}{3g_v}\frac{N_B}{nk_F}$$
$$\times\{C_1\ln(4\varepsilon_F\tau_{sr})+C_2+C_3/\varepsilon_F\tau_{sr}$$
$$+O[(1/\varepsilon_F^2\tau_{sr}^2)]\cdots\}, \quad (38)$$

where C_2 and C_3 depend on L, q_s, and k_F. For $G=0$ and $L=0$ we find $C_1=3/\pi$. The logarithmic singularity in Eq. (38) signals the divergent zero-order result. For $G=0$ and $L\to 0$ we get with Eqs. (22) and (38) the ratio

$$\frac{\tau_t}{\tau_{sr}}=(1+2k_F/q_s)^2\left[\frac{\pi}{3}C_2+\ln(4\varepsilon_F\tau_{sr})\right],$$
$$4\varepsilon_F\tau_{sr}\gg 1. \quad (39)$$

For $1/\varepsilon_F\tau_{sr}\to 0$ we find a logarithmic contribution, which corresponds to our finding that in the case of homogeneous background doping the zero-order result does not exist. Numerical results for τ_t/τ_{sr} versus $\varepsilon_F\tau_{sr}$ (and versus N_B) for homogeneous background doping according to Eqs. (11) and (37c) are shown in Fig. 7. A logarithmic increase of τ_t/τ_{sr} for $1/\varepsilon_F\tau_{sr}\to 0$ is found and reflects the above-mentioned singular behavior. The absolute value of τ_t/τ_{sr} depends on the electron density, see Eq. (39) and the inset in Fig. 7.

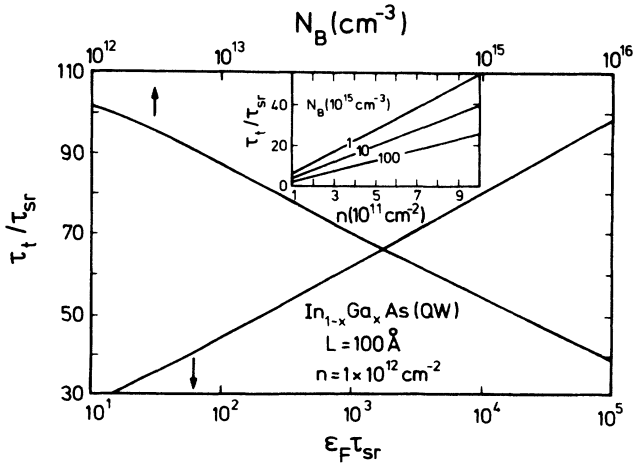

FIG. 7. τ_t/τ_{sr} vs $\varepsilon_F\tau_{sr}$ (lower scale) and vs background doping density N_B (upper scale) for homogeneous background doping in an $In_{1-x}Ga_xAs$ quantum well according to Eqs. (11) and (37c). Results for τ_t/τ_{sr} vs electron density for $N_B=1\times10^{15}$ cm^{-3}, 1×10^{16} cm^{-3}, and 1×10^{17} cm^{-3} are shown in the inset.

Equation (39) is our result for the single-particle relaxation time in the case of homogeneous background doping (for $L\to 0$). In this case τ_s cannot be calculated in the zero-order theory. A self-consistent approach must be used in case of homogeneous background doping (τ_{sr}). From our results on τ_t/τ_s in Sec. III we conclude that for remote-impurity scattering (for $4k_F\alpha\gg 1$), for interface-roughness scattering (for $k_F\Lambda\gg 1$), and for homogeneous background doping (for $N_B\to 0$) a strong enhancement of τ_t/τ_s (or τ_t/τ_{sr}) in comparison to 1 can be achieved.

C. The single-particle relaxation time: long-range potentials

From Eq. (13) one gets for an unscreened interface-roughness scattering potential for $1/\Lambda\to 0$ $[\langle|U(\mathbf{k}-\mathbf{q})|^2\rangle\propto\delta(\mathbf{q}-\mathbf{k})]$ in a quantum well

$$\Sigma(\mathbf{q},z)=2\pi^4\frac{1}{m_z^2}\frac{\Delta^2}{L^6}G(\mathbf{q},z). \quad (40)$$

This result is similar to the result derived for the self-energy of a two-dimensional electron gas in a strong magnetic field.[43] Explicitly we find

$$\Sigma(\mathbf{q},z)=\left[z-\frac{q^2}{2m^*}\right]\Big/2$$
$$\pm\left[\left[z-\frac{q^2}{2m^*}\right]^2\Big/4-2\frac{\pi^4}{m_z^2}\frac{\Delta^2}{L^6}\right]^{1/2}. \quad (41)$$

Equation (41) can be used to calculate the renormalization of the conduction band edge in the presence of interface-roughness scattering.[44] In general $\Sigma(\mathbf{q},z)$ is a complex function with a real and imaginary part. However, in the mass-shell approximation we get $\Sigma(q=k_F, z=\varepsilon_F)'=0$ and $1/\tau_{sr}\equiv 2\Sigma(q=k_F, z=\varepsilon_F)''$ is given by

$$\frac{1}{\tau_{sr}}=2^{3/2}\frac{\pi^2}{m_z}\frac{\Delta}{L^3}. \quad (42)$$

Alternatively we can use Eq. (18) for the calculation of the single-particle relaxation time. We replace in Eq. (18) (q^2-2qk_F) by 0 and obtain for an unscreened interface-roughness scattering potential in a quantum well

$$\frac{1}{\tau_{sr}}=2^{3/2}\frac{\pi^2}{m_z}\frac{\Delta}{L^3}\ , \tag{43}$$

which is the same result as found in Eq. (42) within a different calculation.

We obtain a better approximation if we replace in Eq. (18) $(q^2\mp 2qk_F)^2$ by $4q^2k_F^2$. For a screened long-range interface-roughness potential in a quantum well with $k_F\Lambda \gg 1$ we get

$$\frac{1}{\tau_{sr}}=\frac{1}{\tau_{sr}}2\pi^4\frac{m^{*2}}{m_z^2}\frac{\Delta^2}{L^6q_s^2k_F^2} \times\frac{1+\left[\frac{\Lambda k_F}{8\varepsilon_F\tau_{sr}}\right]^2 e^{(\Lambda k_F/8\varepsilon_F\tau_{sr})^2}\mathrm{Ei}\left[-\left[\frac{\Lambda k_F}{8\varepsilon_F\tau_{sr}}\right]^2\right]}{\{[1-G(2/\Lambda)]F_c(2/\Lambda)+2/\Lambda q_s\}^2} \tag{44a}$$

with

$$\mathrm{Ei}(x)=-\int_{-x}^{\infty}\frac{e^{-t}}{t}dt\ . \tag{44b}$$

Equation (44) is rewritten as

$$\frac{1}{\tau_{sr}}=\varepsilon_F 2^{7/2}\pi^2\frac{m^*}{m_z}\frac{\Delta}{L^3\Lambda q_s k_F^2} \times\frac{\left[1+\sum_{\nu=1}^{\infty}(-1)^{\nu}(\nu+1)!\left[\frac{8\varepsilon_F\tau_{sr}}{\Lambda k_F}\right]^{2\nu}\right]^{1/2}}{\{[1-G(2/\Lambda)]F_c(2/\Lambda)+2/\Lambda q_s\}^1}\ . \tag{45}$$

For $k_F\Lambda \gg 8\varepsilon_F\tau_{sr}$ and with the lowest-order result for $1/\tau_s$ [Eq. (23b)] we get

$$\frac{1}{\tau_{sr}}=\frac{1}{\tau_s}\left[\frac{16\varepsilon_F\tau_s}{\pi^{1/2}k_F\Lambda}\right]^{1/2}\ll\frac{1}{\tau_s}\ . \tag{46}$$

A similar result can be obtained in case of remote-impurity doping for $4k_F\alpha \gg 1$. For $k_F^2/\alpha^2 \ll (m^*/\tau_{sr})^2$ we replace in Eq. (18) $(q^2\mp 2qk_F)$ by 0 and find with τ_s from Eq. (20b)

$$\frac{1}{\tau_{sr}}=\frac{1}{\tau_s}\left[\frac{2\varepsilon_F\tau_s}{k_F\alpha}\right]^{1/2}\ll\frac{1}{\tau_s}\ . \tag{47}$$

We can summarize Eqs. (46) and (47) as follows: as for short-range potentials we get for long-range interface-roughness scattering and for scattering by remote impurities $1/\tau_{sr} \ll 1/\tau_s$.

D. The mobility of $In_{1-x}Ga_xAs$ quantum wells

Analytical results on the mobility, where multiple scattering effects are taken into account, are not available. In Refs. 11, 12, and 16 it was found that multiple scattering effects reduce the mobility in comparison to the lowest-order result [Eq. (11)] and a metal-insulator transition occurs.

Experimental results on the mobility versus electron density of $InP/In_{1-x}Ga_xAs/InP$ quantum wells have been reported recently.[38–42] In Ref. 38 the electron density was varied via the persistent photoeffect.[45] Undoped quantum wells showed a strong increase in the mobility by decreasing the background doping density.[38] In Fig. 8 we show the mobility versus density for scattering from homogeneous background doping, remote-impurity doping (spacer thickness $\alpha=100$ Å) and from alloy disorder scattering. The experimental results for undoped and remote doped quantum wells[38] are also shown in Fig. 8. Experimental details of the quantum wells, used in Ref. 38, are given in Table I. For the solid line in Fig. 8 with $n_i=0$ and $N_B=5\times10^{15}$ cm^{-3} the quantum well width is 150 Å; for the other lines in Fig. 8 we used $L=100$ Å, as in the experiment, see Table I. If we use $\delta V=0.6$ eV, as in Fig. 6, we found that for $n=10^{12}$ cm^{-2} the theoretical mobility is too low. For this reason we used $\delta V=0.5$ eV in Figs. 8 and 9.

The agreement between experiment and theory is acceptable. However, we used a higher background doping level than indicated in Ref. 38 and we assumed that $n_i=$const to get the steep increase of μ versus the electron density (at low n). The dashed line can also explain qualitatively the experimental results of Ref. 40 and is analyzed in more detail.

In Fig. 9 we showed the contribution of the background doping (μ_2) and of the alloy scattering (μ_4) to the mobility (μ_g) versus density, calculated within the lowest-order theory. The dashed lines in Fig. 8 and in Fig. 9 are identical and represent the theory where multi-

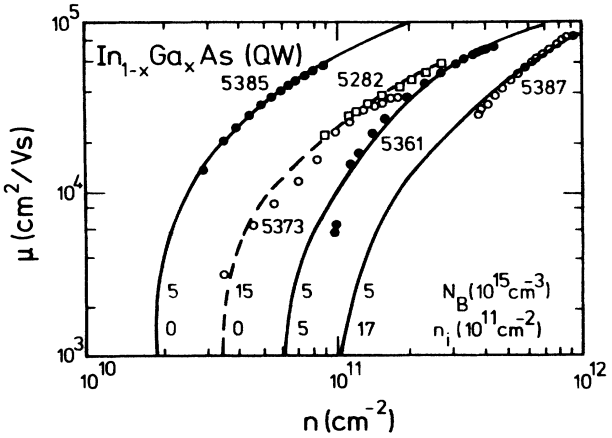

FIG. 8. Mobility μ vs electron density n for an $In_{1-x}Ga_xAs$ quantum well, where three scattering mechanisms are taken into account: remote impurity doping (n_i, $z_i=-100$ Å), homogeneous background doping (N_B), and alloy disorder scattering ($\delta V=0.5$ eV). Multiple scattering effects are included in the theory. The background doping density N_B and the remote impurity density n_i, which we used in the calculation, are indicated. For the solid line with $N_B=5\times10^{15}$ cm^{-3} and $n_i=0$ we used $L=150$ Å. For the other lines we used $L=100$ Å, see text. ●, ○, and □ are experimental results of Ref. 38, see Table I.

TABLE I. Details of the $In_{1-x}Ga_xAs$ quantum wells of Ref. 38.

Structure	Remark	L	Background doping	Remote doping
5385 ●	undoped	150 Å	5×10^{14} cm^{-3}	0
5373 ○	undoped	100 Å	$1-5\times10^{15}$ cm^{-3}	0
5282 □	undoped	100 Å	$1-5\times10^{15}$ cm^{-3}	0
5361 ●	remote	100 Å	$1-5\times10^{15}$ cm^{-3}	10^{17} cm^{-3}
5387 ○	remote	100 Å	$1-5\times10^{15}$ cm^{-3}	5×10^{17} cm^{-3}

ple scattering effects are taken into account. For $n<10^{11}$ cm^{-2} μ_{gr} is significantly smaller than μ_g and multiple scattering effects are important in this density range. A metal-insulator transition occurs for $n=3.5\times10^{10}$ cm^{-2}. It would be very interesting to see whether weak localization effects[23] could explain the experimental results of Ref. 38. In our discussion we neglected interface-roughness scattering. Our theoretical result, shown in Fig. 5, indicates that interface roughness might already be important for $L=100$ Å quantum wells. However, interface-roughness scattering cannot fully account for the mobility of $n<10^{11}$ cm^{-2}, because the ratio of the mobilities for the sample 5385 and the sample 5373 should be $(150/100)^6\approx11$, while from experiment we only find a factor of 5. We believe that the importance of interface roughness scattering could be tested for undoped quantum wells with 60 Å $<L<100$ Å.

E. Renormalized scattering and single-particle relaxation time

Equation (35) is a very important result. Multiple scattering effects increase the single-particle relaxation time and the zero-order result overestimates the effects of disorder. The relevant parameter is $\varepsilon_F\tau_s$. The overestimation is even stronger in the strong coupling regime, see Eq. (34).

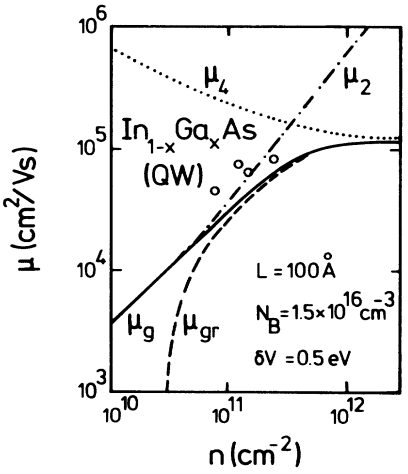

FIG. 9. Mobility μ vs density for homogeneous background doping (μ_2) and alloy disorder scattering (μ_4) for $In_{1-x}Ga_xAs$ quantum wells according to Eq. (11). μ_g is the mobility for both scattering mechanisms. For the dashed line multiple scattering effects have been included. The open circles are experimental results for undoped $In_{1-x}Ga_xAs$ quantum wells from Ref. 40.

In a theory on the metal-insulator transition in disordered electron systems, multiple scattering effects on the scattering time were also taken into account.[11,12,16] An equation similar to Eq. (35) was derived for three-dimensional systems.[46] However, there it was found that the zero-order result underestimates the effects of disorder which would correspond to a minus sign instead of the plus sign on the right-hand side of Eq. (35). This minus sign there signals the metal-insulator transition. The plus sign in Eq. (35) is responsible for the fact that the metal-insulator transition is a dynamic phase transition and is not triggered by singularities of thermodynamic quantities (the compressibility, the density of states); see the exact result for a noninteracting electron gas and for short-range potentials.[47]

Our result for interacting electron systems was derived within the third Klauder approximation;[24] impurity bands were neglected in this approach, see also Refs. 25 and 26. The calculation of the effects of disorder on the single-particle relaxation time provides us with a justification for the assumption made in Refs. 11, 12, and 16, namely, that the effects of disorder on the density of states can be neglected in a crude approach of the metal-insulator transition because disorder does not result in a singular behavior of the density of states.

In Fig. 10 a representative example is shown for remote impurity scattering ($z_i=0$) in Si-MOS systems. We calculated the scattering time τ_{tr}, where multiple scattering effects are included,[12] and τ_t, the lowest-order result [Eq. (11)]. The ratio τ_{tr}/τ_t decreases with decreasing electron density and vanishes at the metal-insulator transition. The ratio of the renormalized single-particle relaxation time τ_{sr}, see Eq. (36), and the lowest-order result of the single particle relaxation time τ_s, see Eq. (19a), increases with decreasing electron density and is 1.14 at the metal-insulator transition.

We conclude from Fig. 10 that $\tau_{tr}/\tau_{sr}<\tau_t/\tau_s$. Multiple scattering effects decrease the ratio of the scattering time and the single-particle relaxation time and at the metal-insulator transition this ratio goes to zero. It is obvious from Fig. 10 that multiple scattering effects are very important for the interpretation of data on τ_t/τ_s in Si-MOS systems and for electron density $n<10^{12}$ cm^{-2}, see Fig. 1 and Refs. 2 and 4. Multiple scattering effects are even more important to a higher impurity density.

Measurements of τ_t and τ_s could help to identify multiple scattering effects, because we see from Fig. 10 that multiple scattering effects lead to much stronger devia-

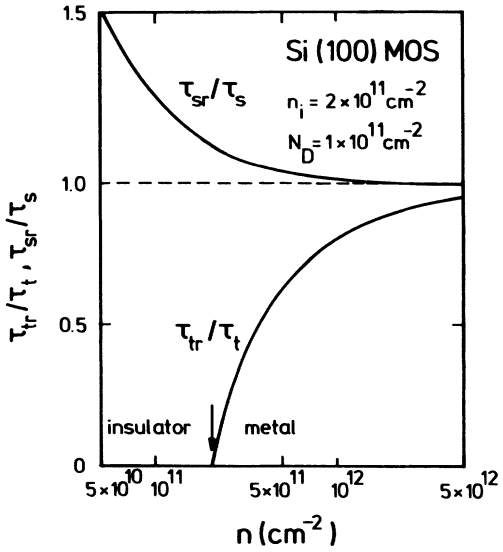

FIG. 10. Results of multiple scattering effects on the scattering time τ_{tr} and the single-particle relaxation time τ_{sr} in a Si-MOS system vs electron density n. τ_t and τ_s represent the lowest-order result according to Eqs. (11) and (16), respectively. The arrow indicates the metal-insulator transition at $n=n_c=2.1\times10^{11}$ cm^{-2}. Remote impurity scattering with $z_i=0$ is considered. τ_{tr} goes to zero for $n\to n_c$.

tions from the lowest-order result in the case of the scattering time than in the case of the single-particle relaxation time.

F. The density of states

The result $\tau_{sr}>\tau_s$ can be explained as follows: one can argue that the lowest-order result overestimates the effects of disorder. However, naively one would expect that multiple scattering effects decrease τ_{sr} in comparison to τ_s in the same way as is the case for the scattering time.

In the mass-shell approximation we get, according to Eq. (14), for the density of states

$$\sigma(\varepsilon_F)=g_v R a^{*2}\left[1/2+\frac{1}{\pi}\arctan(2\varepsilon_F\tau_{sr})\right]. \tag{48}$$

The prefactor on the right-hand side of Eq. (48) is the density of states of the free electron gas $\sigma_0=g_v R a^{*2}$. R is the effective rydberg and a^* the Bohr radius. From Eq. (48) we get

$$\sigma(\varepsilon_F)=\sigma_0\begin{cases}1-\dfrac{1}{2\pi\varepsilon_F\tau_{sr}}, & 2\varepsilon_F\tau_{sr}\gg1\\ 1/2\left[1+\dfrac{4}{\pi}\varepsilon_F\tau_{sr}\right], & 2\varepsilon_F\tau_{sr}\ll1\end{cases} \tag{49}$$

and the density of states is reduced by the finite single-particle relaxation time.

This is due to the fact that for finite disorder the band edge ε_c of the conduction band is shifted from $\varepsilon_c=0$ to $\varepsilon_c<0$. We find

$$\varepsilon_c=-\frac{1}{\tau_{sr}}\begin{cases}(1/12)^{1/2}, & 2\varepsilon_c\tau_{sr}\gg1\\ 4/\pi, & 2\varepsilon_c\tau_{sr}\ll1\end{cases}. \tag{50}$$

The states with $\varepsilon_c<E<0$ are states which were shifted from the $E>0$ energy range to the band tail. We conclude that the density of states in the presence of disorder is lower for $\varepsilon_F>0$ and higher for $\varepsilon_F<0$ than the density of states without disorder. For diverging random potential ε_c goes to minus infinity and $\sigma(\varepsilon_F)$ goes to $\sigma_0/2$. This is the reason why multiple scattering effects increase the density of states in comparison to the lowest-order result and decrease the density of states in comparison to the free-electron gas: $\sigma_s<\sigma_{sr}<\sigma_0$ (index s is for the single-particle relaxation time and index r indicates renormalized). With Fermi's golden rule we get $1/\tau_{sr}\propto\sigma_{sr}$ and $1/\tau_s\propto\sigma_0$ and we conclude $1/\tau_{sr}<1/\tau_s$.

V. CONCLUSION

We have extended the calculation of the single-particle relaxation time for remote-impurity doping[2,6] and short-ranged interface-roughness scattering potentials[2] of a two-dimensional electron gas to long-ranged interface-roughness scattering, alloy disorder scattering, and background impurity scattering.

The lowest-order theory,[2,6] which is linear in the random potential, has been generalized by taking into account multiple scattering effects. Asymptotic results and the corrections to the lowest-order theory have been derived from our self-consistent equations.

$In_{1-x}Ga_xAs$ quantum wells have been discussed in detail by the calculation of the mobility and τ_t/τ_s versus electron density for the various scattering mechanisms and we find that $\tau_t/\tau_s\gg1$ for high electron density and for a long-ranged interface-roughness scattering potential. For homogeneous background doping a logarithmic singularity is found and the self-consistent theory gives $\tau_t/\tau_{sr}\gg1$ for $4\varepsilon_F\tau_{sr}\gg1$, see Eq. (39) and Fig. 7.

We have compared our theory on the mobility in $In_{1-x}Ga_xAs$ quantum wells with recent experimental results[38] and have found good agreement between theory and experiment within reasonable model assumptions. The importance of multiple scattering effects has been pointed out.

ACKNOWLEDGMENTS

I want to thank G. Abstreiter, A. Ghazali, F. Koch, and J. Serre for fruitful discussions. This work has been supported by the Ernst von Siemens Stiftung of the Siemens Aktienqesellschaft.

APPENDIX

1. Alloy scattering

If screening is neglected in the transport theory of alloy scattering, we get with Eqs. (7) and (11) the analytical result

$$\frac{1}{\tau_t}=\varepsilon_F\frac{3}{16}\frac{a^3k_F^2}{L}x(1-x)\left[\frac{\delta V}{\varepsilon_F}\right]^2. \tag{A1}$$

In this approximation the mobility does not depend on the electron density. This result is shown in Fig. 6 as the dotted line. In Ref. 19 the screening for alloy scattering was neglected, but the finite height of the quantum well barrier was considered. Our calculation assumes infinite barriers and is quantitatively correct for quantum wells with $L > 40$ Å. The screening properties of the electron gas increase the mobility in comparison to the unscreened alloy disorder scattering and Fig. 6 demonstrates that screening cannot be neglected.

In Ref. 16 we calculated the parameter A

$$A = \frac{1}{4\pi n^2} \int_0^\infty dq\, q \frac{\langle |U(\mathbf{q})|^2 \rangle}{\epsilon(q)^2} X^0(q)^2 \tag{A2}$$

for various scattering mechanisms. A determines the transport properties of the system.[11,12] For $A < 1$ the electron gas exhibits metallic transport properties and for $A > 1$ the electron gas exhibits a vanishing dc conductivity. In order to get analytical results for alloy disorder scattering we use $q_s \ll 2k_F$, $X^0(q) = \sigma_0 \theta(2k_F - q)$ and get for alloy disorder scattering the critical electron density

$$n_c = \frac{1}{a^{*2}} \frac{3}{32\pi^2} x(1-x) \frac{a^3}{a^{*2} L} g_v \frac{\delta V^2}{R^2} . \tag{A3}$$

For $n > n_c$ the system is a metal. n_c defines the metal-insulator transition. For $In_{1-x}Ga_xAs$ quantum wells we get with $\delta V = 0.6$ eV

$$n_c = (2 \times 10^9 \text{ cm}^{-2}) \left[\frac{100 \text{ Å}}{L} \right]^{1/2} . \tag{A4}$$

2. Three-dimensional systems

According to Eq. (10) we get for three-dimensional systems[7]

$$\frac{1}{\tau_t} = \frac{1}{4\pi\epsilon_F} \int_0^{2k_F} dq\, q^2 \left[\frac{q}{2k_F} \right] \frac{\langle |U(\mathbf{q})|^2 \rangle}{\epsilon(q)^2} . \tag{A5}$$

The single-particle relaxation time in the mass-shell approximation is expressed via Eq. (15) as

$$\frac{1}{\tau_s} = \frac{1}{4\pi\epsilon_F} \int_0^{2k_F} dq\, 2k_F^2 \left[\frac{q}{2k_F} \right] \frac{\langle |U(\mathbf{q})|^2 \rangle}{\epsilon(q)^2} . \tag{A6}$$

For charged impurity scattering with $\langle |U(\mathbf{q})|^2 \rangle = n_i (4\pi e^2/\epsilon_L q^2)^2$ and the screening function in the Thomas-Fermi approximation $\epsilon(q) = 1 + q_s^2/q^2$ we get the Mott-Jones formula for the scattering time.[48] The ratio τ_t/τ_s [see Eqs. (A5) and (A6)] can be calculated analytically and is expressed as

$$\frac{\tau_t}{\tau_s} = 8 \frac{y^4}{1+4y^2} \frac{1}{\ln(1+4y^2) - 4y^2/(1+4y^2)} \tag{A7}$$

and $y = k_F/q_s$. The asymptotic result of Eq. (A7) is written as

$$\frac{\tau_t}{\tau_s} = \begin{cases} 1 + 4y^2/3, & y \ll 1 \\ 1.97, & y = 1 \\ 2y^2/\ln(1+4y^2), & y \gg 1 . \end{cases} \tag{A8}$$

Equation (A7) was shown in Fig. 1 of Ref. 6.

*Present address.

[1] T. Ando, A. B. Fowler, and F. Stern, Rev. Mod. Phys. **54**, 437 (1982).

[2] J. P. Harrang, R. J. Higgins, R. K. Goodall, P. R. Jay, M. Laviron, and P. Delescluse, Phys. Rev. B **32**, 8126 (1985).

[3] A. Gold and W. Götze, J. Phys. C **14**, 4049 (1981).

[4] F. F. Fang, A. B. Fowler, and A. Hartstein, Phys. Rev. B **16**, 4446 (1977).

[5] M. A. Paalanen, D. C. Tsui, and J. C. M. Hwang, Phys. Rev. Lett. **51**, 2226 (1983).

[6] S. Das Sarma and F. Stern, Phys. Rev. B **32**, 8442 (1985).

[7] A. A. Abrikosov, L. P. Gorkov, and I. E. Dzyaloshinski, *Methods of Quantum Field Theory in Statistical Physics*, (Prentice-Hall, Englewood Cliffs, NJ, 1963), Sec. 39.

[8] F. F. Fang, T. P. Smith III, and S. L. Wright, Surf. Sci. **196**, 310 (1988).

[9] P. G. de Gennes, J. Phys. Radium **23**, 630 (1962).

[10] T. Ando, J. Phys. Soc. Jpn. **51**, 3215 (1982).

[11] W. Götze, Solid State Commun. **27**, 1393 (1978); A. Gold and W. Götze, Helv. Phys. Acta **56**, 47 (1983).

[12] A. Gold and W. Götze, Phys. Rev. B **33**, 2495 (1986).

[13] F. Stern and W. E. Howard, Phys. Rev. **163**, 816 (1967).

[14] A. Gold, Phys. Rev. B **35**, 723 (1987).

[15] Y. Matsumoto and Y. Uemura, in Proceedings of the Second International Conference on Solid Surfaces, Kyoto, 1974 [Jpn. J. Appl. Phys. Suppl. **2**, Pt. 2, 367 (1974)].

[16] A. Gold, Solid State Commun. **60**, 531 (1986).

[17] T. Ando, J. Phys. Soc. Jpn. **51**, 3900 (1982).

[18] P. K. Basu and B. R. Nag, Appl. Phys. Lett. **43**, 689 (1983); G. Bastard, *ibid.* **43**, 531 (1983).

[19] J. A. Brum and G. Bastard, Solid State Commun. **53**, 727 (1985).

[20] F. Stern, Phys. Rev. Lett. **18**, 546 (1967).

[21] M. Jonson, J. Phys. C **9**, 3055 (1976).

[22] J. Lindhard, K. Dan. Vidensk. Selsk., Mat. Fys. Medd. **28**, 1 (1954).

[23] For a review see P. A. Lee and T. V. Ramakrishnan, Rev. Mod. Phys. **57**, 287 (1985).

[24] J. R. Klauder, Ann. Phys. (N.Y.) **14**, 43 (1961).

[25] J. Serre and A. Ghazali, Phys. Rev. B **28**, 4704 (1983).

[26] A. Gold, J. Serre, and A. Ghazali, Phys. Rev. B **37**, 4589 (1988).

[27] A. Gold and V. T. Dolgopolov, Phys. Rev. B **33**, 1076 (1986).

[28] P. J. Price, J. Vac. Sci. Technol. **19**, 599 (1981).

[29] Equation (22) differs from Eq. (13) of Ref. 14 by the factor $2/\pi$ and is an improved expression for $1/\tau_t$.

[30] J. H. English, A. C. Gossard, H. L. Störmer, and K. W. Baldwin, Appl. Phys. Lett. **50**, 1826 (1987).

[31] A. Gold, Phys. Rev. B **32**, 4014 (1985).

[32] E. Glaser, R. Czaputa, B. D. Mc.Combe, Solid State Commun. **54**, 715 (1985).

[33] A. Gold, Surf. Sci. **170**, 381 (1986).

[34]T. Ando, J. Phys. Soc. Jpn. **51**, 3900 (1982).
[35]H. Sakaki, T. Noda, K. Hirakawa, M. Tanaka, and T. Matsusue, Appl. Phys. Lett. **51**, 1934 (1987).
[36]R. Gottinger, A. Gold, A. Abstreiter, G. Weimann, and W. Schlapp, Europhys. Lett. **6**, 183 (1988).
[37]K. Hirakawa and H. Sakaki, Phys. Rev. B **33**, 8291 (1986).
[38]D. A. Anderson, S. J. Bass, M. J. Kane, and L. L. Taylor, Appl. Phys. Lett. **49**, 1360 (1986).
[39]W. T. Tsang and E. F. Schubert, Appl. Phys. Lett. **49**, 220 (1986).
[40]M. Frei, D. C. Tsui, and W. T. Tsang, Appl. Phys. Lett. **50**, 606 (1987).
[41]L. L. Taylor, M. J. Kane, and S. J. Bass, Appl. Phys. Lett. **51**, 180 (1987).
[42]M. Zachau, P. Helgesen, F. Koch, D. Grützmacher, H. Jürgensen, and P. Balk (unpublished).
[43]For a review see Ref. 1.
[44]A. Gold (unpublished).
[45]H. L. Störmer, R. Dingle, A. C. Gossard, W. Wiegmann, and M. D. Sturge, Solid State Commun. **29**, 705 (1979).
[46]W. Götze, Philos. Mag. B **43**, 219 (1981).
[47]F. Wegner, Z. Phys. B **44**, 9 (1982).
[48]See, J. M. Ziman, *Principles of the Theory of Solids* (Cambridge University Press, Cambridge, 1972).